Double-link expandohedra: a mechanical model for expansion of a virus

By F. Kovács[1], T. Tarnai[2], S.D. Guest[3] and P.W. Fowler[4]

[1]*Research Group for Computational Structural Mechanics, Hungarian Academy of Sciences, Budapest, Műegyetem rkp. 3., H-1521 Hungary*
[2]*Department of Structural Mechanics, Budapest University of Technology and Economics, Budapest, Műegyetem rkp. 3., H-1521 Hungary*
[3]*Department of Engineering, University of Cambridge, Trumpington Street, Cambridge CB2 1PZ, UK*
[4]*Department of Chemistry, University of Exeter, Stocker Road, Exeter EX4 4QD, UK*

Double-link expandohedra are introduced: each is constructed from a parent polyhedron by replacing all faces with rigid plates, adjacent plates being connected by a pair of spherically jointed bars. Powerful symmetry techniques are developed for mobility analysis of general double-link expandohedra, and when combined with numerical calculation and physical model building, demonstrate the existence of generic finite breathing expansion motions in many cases. For icosahedrally symmetric trivalent parents with pentagonal and hexagonal faces only (fullerene polyhedra), the derived expandohedra provide a mechanical model for the experimentally observed swelling of viruses such as cowpea chlorotic mottle virus (CCMV). A fully symmetric swelling motion (a finite mechanism) is found for systems based on icosahedral fullerene polyhedra with odd triangulation number, $T \leq 31$, and is conjectured to exist for all odd triangulation numbers.

Keywords: Symmetry; Polyhedra; Mechanism; Virus Structures

1. Introduction

Many viruses consist of an outer protein coat (the virion) containing a DNA or RNA 'payload', where the virion undergoes reversible structural changes that allow switchable access to the interior by the opening of interstices through expansion. These changes may be driven, for example, by variations in pH of the biological medium. The present paper introduces a mechanical model that helps to understand the expansion in terms of classical principles of structural mechanics.

An example that has been well characterised is the cowpea chlorotic mottle virus (CCMV), shown in figure 1, that has a structure based on the truncated icosahedron ('$T = 3$' in the standard notation for triangulated icosahedral structures (Caspar & Klug 1962)). In the native form, stable around pH 5, 180 chemically identical protein subunits form a shell of diameter $\simeq 286$ Å. The protein subunits form into either pentagonal or hexagonal capsomeres. At pH 7, the virus particles undergo a 10% increase in radius, thought to occur as a result of deprotonation of carboxyl moieties at the inter-capsomere contacts, leading to electrostatic repulsion that opens out the

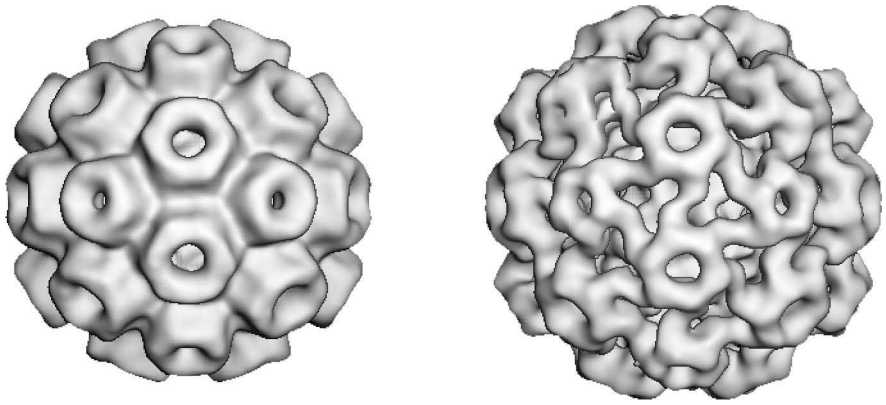

(a) (b)

Figure 1. Cryoelectron microscopy and image reconstruction of the cowpea chlorotic mottle virus (CCMV): (a) in an unswollen condition induced by low pH; (b) in a swollen condition induced by high pH. Images provided by T. Baker, Purdue University.

structure but falls short of complete disassembly through preservation of interwoven carboxyl/protein links between capsomeres (Speir *et al.* 1995). Discrete swollen states have also been observed in many plant viruses, e.g. turnip crinkle (Sorger *et al.* 1986), tomato bushy stunt (Robinson & Harrison 1982) and southern bean mosaic viruses (Rayment *et al.* 1979), and similar phenomena have been inferred for animal viruses such as poliovirus (Fricks & Hogle 1990). An important feature of the swelling process is that it leads to opening of a 20 Å-diameter portal on the quasi-threefold axes at full expansion. Exploitation of these portals for pH-gated material transport and fabrication of mineralised nanoparticles has been proposed (Douglas & Young 1998, 1999).

In engineering terms, virion expansion can be considered as the actuation of an expandable-retractable nanostructure. Expanding structures on the macroscopic scale have been well studied with a view to exploitation e.g. as deployable structures (Pellegrino & Guest, 2000). Kovács *et al.* (2003) introduced a class of expandable polyhedral structures, the expandohedra, consisting of prismatic faces with a single link along each edge formed by hinged plates. The existence of a finite breathing motion for such systems depends critically on the correct geometry of the linking hinge assembly. The geometry of this single-link prototype differs in detail from that found in viruses: the experimental observations on (Speir *et al.* 1995) show a linkage where adjacent 'faces' have a double-link connection exhibiting local C_2 symmetry.

The present paper shows that it is possible to adapt the notion of an expandohedron to the biological context by constructing a double-link expandohedron with several desirable properties. Not only is the double-link structure closer to the observed virus morphology, while retaining a finite breathing mode, but the existence of this mode is a generic symmetry feature that does not depend on a particular linkage *geometry*. The links consist of a pair of bars connected to the faces by

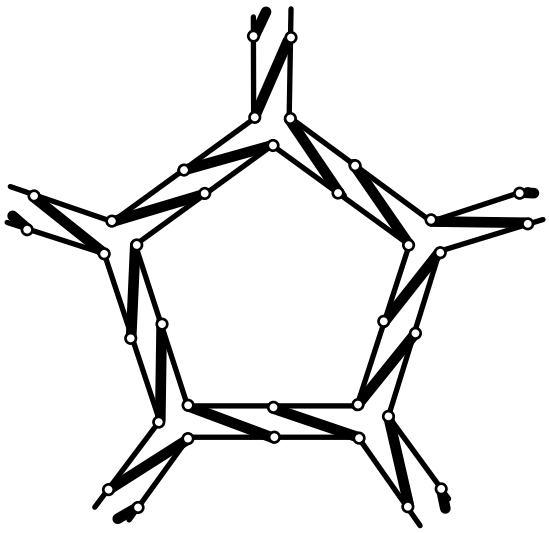

Figure 2. The construction of a double-link expandohedron around a regular pentagonal face. A simple arrangement, in which links run from vertices to edge mid-points, is shown; many other arrangements are compatible with the construction described in the text.

spherical joints, in a simplified form of a double link suggested in the concluding paragraph of the paper by Kovács *et al.* (2003).

2. Construction

We will consider double-link expandohedra based on trivalent polyhedral parents, i.e. polyhedra in which each vertex is the meeting point of three edges. These include as special cases all the 'fullerenes', which consist entirely of hexagonal and pentagonal faces, the latter being twelve in number, and in particular icosahedral fullerenes, which are possible for vertices numbering $20T$, where T is the *triangulation number*, defined as $T = i^2 + ij + j^2$ such that $i, j = 0, 1, 2, ...,\ i^2 + j^2 \neq 0$ (Coxeter 1971; Goldberg 1937). These icosahedral fullerenes provide structural models for a large class of viruses (Caspar & Klug 1962).

Consider a trivalent polyhedron P. The double-link expandohedron D is constructed from the elements of P as shown schematically in figure 2. First the faces of P are separated. D contains a distinct rigid prism for each face of P, the same in size and shape as the original. Each edge of P is thereby doubled, with the edge that was common to two faces now replaced by edges of the separated faces. The rigid face prisms are now linked by a pair of bars that are connected to the prisms by spherical joints: these bars run 'diagonally' across the gap. The choice of sense of diagonals is made cyclically on some starting face, and then propagated consistently over the whole set of face prisms.

The construction described gives a 'fully closed' configuration, where the bars along an edge are both co-linear with the edge. However, a more general initial geometric configuration would be given by initially displacing the face prisms in some way consistent with the symmetry of D, and then generating the bars. There

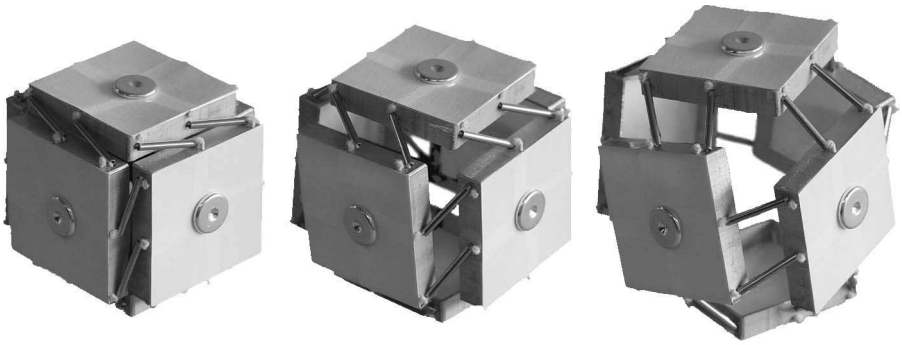

Figure 3. A double-link expandohedron based on the cube; the model is shown expanding from left to right. The faces consist of square-box sections; the linking bar is a tube containing a prestressed elastic string running face to face. The method of construction leads to the structure being most relaxed in its expanded state, from which it can be closed by drawstrings running between opposite faces. The drawstrings have been edited out of these images, for clarity.

is a great deal of latitude in the placement of the bars; to reproduce a morphology similar to that seen in virus structures, each would run approximately from a vertex on one face to the midpoint of the adjacent face. In CCMV for example, the linking protein strands, modelled here by spherically-jointed bars, are anchored *within* the capsomere subunits. The only conditions that the bar placement *must* follow are that the disposition of the bars should respect any rotational symmetries of P, and the bars must not coincide.

An example of a physical model of a double-link expanding cube constructed as described is shown in figure 3.

3. Mobility analysis

(*a*) *Mobility counting*

In our mobility analysis, we shall consider each of the bars between faces to provide a single constraint on the motion of the faces. Thus we will not consider the bars separately as rigid bodies. By construction then, D consists of f rigid bodies and $2e$ constraints, where f and e are respectively the numbers of faces and edges of P, which are related to v, the number of vertices of P, by the Euler relation for spherical polyhedra, $v+f=e+2$. As P is trivalent, $e=3v/2$, and $f=v/2+2$.

The mobility criterion is a simple generic counting relationship for calculating the degrees of freedom of a mechanical linkage (Hunt 1978). In a form that allows for non-independent constraints (Guest & Fowler 2003) the mobility of a linkage consisting of n bodies connected by g joints, where joint i provides c_i constraints, is given by

$$m - s = 6(n-1) - \sum_{i=1}^{g} c_i, \tag{3.1}$$

where m is the number of mechanisms and s is the number of states of self-stress

that the linkage can sustain (a state of self-stress is a set of internal forces in the linkage in equilibrium with zero external load).

Here each face is a rigid body, so $n = f$, and for each of the $g = e$ sets of links between faces, $c_i = 2$, i.e. there are two constraints per edge of P. Thus

$$m - s = 6(f - 1) - 2e \tag{3.2}$$

and, for a trivalent parent polyhedron P,

$$m - s = 6(v/2 + 1) - 3v = 6. \tag{3.3}$$

Thus, every double-link expandohedron based on a trivalent polyhedron has at least six mechanisms. Simple counting gives no information about the nature of these mechanisms; they may be finite or infinitesimal, and may or may not include a fully symmetric breathing mode. A symmetry analysis will help to clarify these issues.

(*b*) *A symmetry-extended mobility analysis*

This section will use a symmetry-extended mobility rule written in the language of *representations*. The representation of a set of objects, such as faces or constraints, denoted by Γ(object), describes the symmetry of that set in the relevant point group, which here is the rotational subgroup $G(D)$ of $G(P)$, the full point group of P. The representation Γ(object) collects the *character* $\chi(S)$ of a set under a symmetry operation S, i.e. the trace of the matrix that relates the set before and after the application of S.

In the language of representations, one form of the mobility criterion (Guest & Fowler 2003) is

$$\Gamma(m) - \Gamma(s) = \Gamma(\text{relative body freedoms}) - \Gamma(\text{constraints}) \tag{3.4}$$

where $\Gamma(m)$ and $\Gamma(s)$ are the representations of the mobilities, and the states of self-stress, respectively. Following the development in Guest & Fowler (2003), the relative body freedoms of D span

$$\Gamma(\text{relative body freedoms}) = (\Gamma_\sigma(f, P) - \Gamma_0) \times (\Gamma_T + \Gamma_R) \tag{3.5}$$

where $\Gamma_\sigma(f, P)$ is the permutation representation of the face centres of P, Γ_0 is the totally symmetric representation, and Γ_T and Γ_R are the translation and rotational representations, all in the point group $G(D)$. This is a mathematical expression of the fact that, in the absence of constraints, each body can rotate and translate independently in 3D space.

In D, each bar imposes a scalar constraint on the distance between points on the connected rigid face prisms. For each edge these scalar constraints have an in-phase and out-of-phase combination. The in-phase component spans $\Gamma_\sigma(e, P)$, the permutation representation of the edge centres of P, and the out-of-phase component spans $\Gamma_\rightarrow(e, P)$, the representation of a set of vectors along the edges of P. Hence, the set of all constraints spans

$$\Gamma(\text{constraints}) = \Gamma_\sigma(e, P) + \Gamma_\rightarrow(e, P). \tag{3.6}$$

In total, substituting (3.5) and (3.6) into (3.4), and noting that $\Gamma_R = \Gamma_T$ in the pure rotational group $G(D)$,

$$\Gamma(m) - \Gamma(s) = 2(\Gamma(f,P) - \Gamma_0) \times \Gamma_T - \Gamma_\sigma(e,P) - \Gamma_\rightarrow(e,P). \tag{3.7}$$

Further simplification is possible by taking the symmetry relations for structural components of trivalent polyhedra (Ceulemans & Fowler 1991) in versions appropriate to a pure rotational group:

$$\Gamma_\sigma(f,P) + \Gamma_\sigma(v,P) = \Gamma_\rightarrow(e,P) + 2\Gamma_0, \tag{3.8}$$

$$\Gamma_\sigma(v,P) \times \Gamma_T = \Gamma_\rightarrow(e,P) + \Gamma_\sigma(e,P), \tag{3.9}$$

$$\Gamma_\sigma(e,P) \times \Gamma_T = \Gamma_\sigma(e,P) + 2\Gamma_\rightarrow(e,P) \tag{3.10}$$

where $\Gamma_\sigma(v,P)$ is the permutation representation of the vertices of P. Multiplying (3.8) by $2\Gamma_T$, using (3.9) to replace $\Gamma_\sigma(v,P) \times \Gamma_T$ and replacing $2\Gamma_\rightarrow(e,P)$ from (3.10) by $\Gamma_\sigma(e,P) \times \Gamma_T - \Gamma_\sigma(e,P)$ allows (3.7) to be written, for P trivalent, as

$$\Gamma(m) - \Gamma(s) = \Gamma_\sigma(e,P) \times \left\{ \Gamma_T \times \Gamma_T - \frac{5}{2}\Gamma_T - \frac{3}{2}\Gamma_0 \right\} + 2\Gamma_T. \tag{3.11}$$

The mathematical form of (3.11) has a number of useful consequences. The first observation to note is that the term in braces has character $3 \times 3 - 3 \times 5/2 - 3/2 = 0$ under the identity operation, so that the results $m - s = 6$ of the scalar counting rule is recovered. The second observation is that the right-hand side of (3.11) consists of a term that depends on the structure of P, $\Gamma_{\text{structure}}$, and a term $(2\Gamma_T)$ that does not. The third observation is that the P-dependent term has character zero under every operation except those C_2 rotations whose axes pass through edges of P; $\Gamma_\sigma(e,P)$ has non-vanishing character only such C_2 operations and the identity, and the term in braces has zero character under the identity, as noted above. As $\Gamma_T \times \Gamma_T - (5/2)\Gamma_T - (3/2)\Gamma_0$ has character $+2$ under all C_2 operations, we can write, for P trivalent,

$$\Gamma(m) - \Gamma(s) = \Gamma_{\text{structure}} + 2\Gamma_T \tag{3.12}$$

where $\Gamma_{\text{structure}}$ has character zero everywhere but under operation $S = C_2$, where the character is $2x$, with x the number of edges of P unshifted by S (zero, one or two). For any particular case, reduction of $\Gamma_{\text{structure}}$ is straightforward, particularly if there is only one class of C_2 operations. However, even these simple calculation can be avoided, as (3.12) has a solution in closed form for all possible groups.

(*c*) *Mobility by symmetry group*

A complete solution of (3.12) can be given for all double-link expandohedra based on trivalent parents. The twisted nature of the links in D implies that $G(D)$ is a pure rotational point group, and is hence limited to five possibilities: an axial group C_N, a dihedral group D_N, the tetrahedral group T, the octahedral group O, or the icosahedral group I. All trivalent polyhedra P, whatever their full point group $G(P)$, produce a double-link expandohedron belonging to one of these five

symmetry types. $G(D)$ is the maximum rotational subgroup, obtained by striking out all improper operations from $G(P)$; the full set of possibilities is:

$$\begin{aligned} G(P) \to G(D): \quad C_{Nv}, C_{Nh}, S_{2N}, C_N &\to C_N, \\ D_{Nh}, D_{Nd}, D_N &\to D_N, \\ T_h, T_d, T &\to T, \\ O_h, O &\to O, \\ I_h, I &\to I. \end{aligned}$$

For all double-link expandohedra based on trivalent parents, the symmetry difference between mechanisms and states-of-self-stress is governed entirely by the numbers of edges that lie on C_2 axes, and (3.11) therefore reduces to a simple formula for $\Gamma(m) - \Gamma(s)$. The procedure is to reduce $\Gamma_{\text{structure}}$ to a sum of irreducible components. As the only characters of $\Gamma_{\text{structure}}$ that may take non-zero values are those for C_2 operations, the number of occurrences of a given irreducible representation Γ_i is

$$\frac{2\, n_2\, x\, \chi_i(C_2)}{|G|}$$

where n_2 is the number of C_2 operations in the class, $\chi_i(C_2)$ is the character of Γ_i and $|G|$ is the order of the group. Reduction of Γ_T is shown in standard tables (Atkins *et al.* 1970).

The results fall naturally into eight subcases:

$G(D) = I$: The number of edges on a C_2 axis is either $x = 2$ or $x = 0$, and

$$\Gamma(m) - \Gamma(s) = \frac{x}{2}(A - T_1 - T_2 + H) + 2T_1; \tag{3.13}$$

$G(D) = O$: The number of edges on a C_2 axis that coincides with a principal C_4 axis must be $x = 0$, and on any other C_2 axis is either $x = 2$ or $x = 0$. Thus

$$\Gamma(m) - \Gamma(s) = \frac{x}{2}(A_1 - A_2 - T_1 + T_2) + 2T_1; \tag{3.14}$$

$G(D) = T$: The number of edges on a C_2 axis is either $x = 2$ or $x = 0$, and

$$\Gamma(m) - \Gamma(s) = \frac{x}{2}(A + E - T) + 2T; \tag{3.15}$$

$G(D) = D_2$: The numbers of edges, x, y, z, on the three distinct C_2 axes can each independently take values of 2 or 0. Thus

$$\begin{aligned} \Gamma(m) - \Gamma(s) = \frac{1}{2}(x + y + z)A + \frac{1}{2}(4 - x - y + z)B_1 + \\ \frac{1}{2}(4 - x + y - z)B_2 + \frac{1}{2}(4 + x - y - z)B_3; \end{aligned} \tag{3.16}$$

$G(D) = D_N$, $N > 2$, N even: The number of edges on the C_2 axis that coincides with the principal C_N axis is $x = 0$, and the numbers of edges, x', x'', on the

distinct transverse C_2' and C_2'' axes each independently take values of 2 or 0. Thus

$$\Gamma(m) - \Gamma(s) = \frac{1}{2}(x' + x'')A_1 + \frac{1}{2}(4 - x' - x'')A_2 + \frac{1}{2}(x' - x'')B_1 + \frac{1}{2}(x'' - x')B_2 + 2E_1, \quad (3.17)$$

(where $E_1 \equiv E$ for $N = 4$);

$G(D) = D_N$, N odd: The number of edges on a C_2 axis is one of $x = 2, 1, 0$, and

$$\Gamma(m) - \Gamma(s) = xA_1 + (2 - x)A_2 + 2E_1, \quad (3.18)$$

(where $E_1 \equiv E$ for $N = 3$);

$G(D) = C_2$: The number of edges on the C_2 axis can take values of $x = 2, 1, 0$, and

$$\Gamma(m) - \Gamma(s) = (2 + x)A + (4 - x)B; \quad (3.19)$$

$G(D) = C_N$, $N \neq 2$: There is no pure C_2 axis, and

$$\Gamma(m) - \Gamma(s) = 2\Gamma_T, \quad (3.20)$$

where $2\Gamma_T = 6A$ for $N = 1$, $2\Gamma_T = 2A + 2E$ for $N = 4$, and $2\Gamma_T = 2A + 2E_1$ otherwise.

It will later prove useful to have noted that $\Gamma(m) - \Gamma(s)$ contains the totally symmetric representation for any double-link expandohedron D where at least one edge of the parent polyhedron lies on a C_2 axis, and for any D where $G(D)$ is an axial C_N group. This implies that $\Gamma(m)$ contains a totally symmetric component, and therefore that the structure has a totally symmetric mechanism — either infinitesimal or finite. Subsection 3(e) discusses how to determine when this mechanism is a finite breathing mode.

(*d*) *Icosahedral virus systems*

The structures of interest as models of viruses are the trivalent polyhedra defined by $T = i^2 + ij + j^2$ such that $i, j = 0, 1, 2, ...$, $i^2 + j^2 \neq 0$, and consist of an icosahedral arrangement of 12 pentagons and $10(T - 1)$ hexagons, having $20T$ vertices and therefore $30T$ edges. These are precisely the polyhedra that represent icosahedrally-symmetric fullerene carbon cages, and are the icosahedral members of the class of 'multi-symmetric' polyhedra (Goldberg 1937). For these systems, the results of §3(c) can be extended.

A chiral icosahedral fullerene polyhedron has orbits of edges of sizes 30 or 60, where two edges of an orbit of size 30 lie on each C_2 axis ($x = 2$), but no edges on an orbit of size 60 lie on any C_2 axis ($x = 0$). It has vertices that fall into orbits of 20 (vertices on C_3 axes), and orbits of 60 (vertices in the general position). Edge orbits of size 20 are not possible, as a tangential edge may not have C_3 symmetry, and vertex orbits of size 30 are likewise forbidden by the impossibility of C_2 symmetry for a vertex at the junction of three tangential edges. A single-shell icosahedral

fullerene polyhedron can therefore have at most one 30 orbit, since the edges that make up the 30 orbit occupy all the points at which the 15 C_2 axes pierce the sphere, and therefore this orbit can be occupied only if T is odd. $T = 4$ (the 80 vertex icosahedral fullerene) is the smallest case with $x = 0$.

Similarly, the single-shell icosahedral fullerene polyhedron can have at most one 20-orbit of vertices, with the same necessary and sufficent condition that T be odd. Hence $x = 0$ iff T is even, and $x = 2$ iff T is odd. Thus there is a guaranteed totally symmetric mechanism iff T is odd, valid in particular for $T = 1$ and all of its successive leapfrogs (Fowler & Steer 1987) $T = 3, 9, 27, ...$

The result generalises to the other Goldberg polyhedra, the tetrahedrally symmetric trivalents with 4 triangles, and the octahedrally symmetric trivalents with 6 squares, all other faces being hexagonal. In these cases the vertex counts are $4T$ and $8T$, the edge counts $6T$ and $12T$, and the $x = 2$ case is exactly that of a polyhedron with a single 6 (12) orbit of edges, i.e. T odd.

Orbit analysis can also be applied to the parameters determining bar positions in double-link expandohedra. For example in the case $T = 3$ links may be constructed with three distinct bar lengths, two for pentagon-hexagon contacts, and one for the hexagon-hexagon contacts on the C_2 axis. This allows tuning of the model to reproduce experimentally observed features such as the pentamer 'dimpling' of the swollen CCMV (Speir *et al.* 1995).

(*e*) *A finite breathing mode?*

Kangwai and Guest (1999) gave two conditions that together guarantee that a mechanism is finite and not only infinitesimal. These are that the mechanism has to be totally symmetric in some appropriate symmetry group, while at the same time there must *not* be a totally symmetric state of self-stress. The previous section showed that many double-link expandohedra are certain to have a totally symmetric mechanism from a mobility analysis; this section will determine under which conditions it can be guaranteed that a totally symmetric state of self-stress does not exist.

A totally symmetric state of self-stress can be ruled out for almost all configurations of double-link expandohedra based on the five platonic solids. Here, every edge has a C_2 axis passing through it, and for a totally symmetric state of self-stress, if there is a tension in one bar linking two faces, there must be an equal tension in the other bar. Considering one of the faces, these tensions will have a component perpendicular to the face, except when both bars lie parallel to the face, which can only happen in the fully closed configuration. As all pairs of bars on each edge of a face provide the same force, the face can only be in equilibrium in the fully closed configurations, or if the tensions are both zero. Thus apart from the fully closed configuration, there can be no totally symmetric state of self-stress. Arguments based on vertex parity show that even for the fully closed configuration, only the octahedron can support a totally symmetric state of self-stress.

The simple result above that a totally symmetric state of self-stress is not possible in a generic configuration does not extend to icosahedral fullerene polyhedra. For a general placement of bars, however, numerical calculation (§4) has not found a totally symmetric state of self-stress for cases of interest.

Additional, not totally symmetric, states of self-stress in the fully closed configuration exist for any expandohedron. There will always be a 'local' state of self-stress where one bar of an edge is in tension, and the other is in compression. Thus in the fully closed state, the states of self-stress must span at least $\Gamma_{\rightarrow}(e, P)$, and to preserve $\Gamma(m) - \Gamma(s)$ there must be additional mechanisms, which disappear once the double-link expandohedron is displaced along its totally symmetric breathing mode.

4. Calculations

Two types of calculation were carried out. Firstly, detailed symmetry-adapted calculations to characterise mechanisms and states of self-stress were carried out for double-link expandohedra based on each of the trivalent platonic solids. Secondly, a more limited check on the number of mechanisms and states of self-stress was made for the first 15 icosahedral expandohedra.

(*a*) *Platonic double-link expandohedra*

In each case, a 'general' geometry is found by initially forming the expandohedra in its fully closed state, with bars running from vertices to edge mid-points. Each face is then rotated about its normal by 10°, and displaced along its normal by the distance required to restore the correct bar lengths. For this geometry, a symmetry-adapted equilibrium matrix (Kangwai & Guest 2000) is calculated, and used to characterise states of self-stress and mechanisms. The results are as follows:

Dodecahedron, $G(D) = I$:

$$m = 9; \quad s = 3, \tag{4.1}$$

$$\Gamma(m) = A + T_1 + H; \quad \Gamma(s) = T_2; \tag{4.2}$$

Cube, $G(D) = O$:

$$m = 7; \quad s = 1, \tag{4.3}$$

$$\Gamma(m) = A + T_1 + T_2; \quad \Gamma(s) = A_2; \tag{4.4}$$

Tetrahedron, $G(D) = T$:

$$m = 6; \quad s = 0, \tag{4.5}$$

$$\Gamma(m) = A + E + T; \quad \Gamma(s) = 0. \tag{4.6}$$

For each of these cases, there are two edges on each C_2 axis, and hence $x = 2$, and the symmetry results (3.13)–(3.15) give a full account of the mechanisms and states of self-stress. In particular, there is no totally symmetric state of self-stress.

(*b*) *Icosahedral double-link expandohedra*

Calculations were carried out for the double-link expandohedra based on the icosahedral fullerene polyhedra, $T = 1$, 3, 4, 7, 9, 12, 13, 16, 19, 21, 25, 27, 28, 31, 36, i.e. the first 15 possibilities. In each case a 'generic' geometry was constructed by taking 'topological coordinates' from the eigenvectors of the adjacency matrix (Manolopoulos & Fowler 1992), separating the faces by radial expansion of 10%,

concerted rotation of all faces by 3°, and connection of bars between vertices and edge mid-points. These coordinates have the full (chiral) symmetry $G(D)$, but are otherwise essentially arbitrary. An equilibrium matrix relating the forces and couples applied to faces, to the tension in the linking bars was constructed, and its rank determined. The dimensions and the rank of this matrix give the number of mechanisms and states of self-stress (Pellegrino 1993).

The idea behind using a single point calculation of this kind is that the symmetry-mobility criterion is derived for a generic geometry within the appropriate symmetry-group, and as such give a minimum, but not necessarily complete, account of the mechanism and states of self-stress. Examples are known where such a result is incomplete for special configurations (Fowler & Guest 2000), or displays systematic incompleteness for all configurations (Fowler & Guest 2002). In the present case either is *a priori* conceivable, but can be distinguished by an appropriate single-point calculation if this shows that the minimum set is complete at some 'generic' single point. A single-point calculation that shows the minimum set is incomplete does not distinguish between the cases. For example, if a double-link expandohedron for $T = 4$ was constructed as above, but without face rotation, it would give $m = 15$, $s = 9$, but here edges of adjacent faces are parallel, as are the connecting bars.

The 15 results follow a simple pattern. The odd values of T give $m = 9$ and $s = 3$, whereas the even values of T give $m = 6$ and $s = 0$. As these are exactly the number predicted by the symmetry mobility criterion (3.11), we see that symmetry gives a full account of the mechanisms and states of self-stress in the generic icosahedrally symmetric configuration. Application of (3.13) tells us that the mechanisms for T odd span $A+T_1+H$, and for T even span $2T_1$, whereas the states of self-stress span the representation T_2 for odd T, and are absent for even T. Thus the mobilities of all odd T cases, including that of the CCMV, follow the pattern set by $T = 1$, the dodecahedron (4.2). It is a natural conjecture that these results are true for all T.

5. Conclusions

This paper has introduced an infinite class of *double-link expandohedra*, each constructed from a parent polyhedron by replacing all faces with rigid plates, and connecting adjacent plates with a pair of spherically jointed bars. The construction is a realistic model of observed morphology of e.g. CCMV and other viruses capable of reversible expansion under change in pH.

New symmetry-based techniques have been used to provide a general account of the mobility of such expandohedra, giving closed formulae for the symmetry excess of mechanisms over states of self stress for all the possible double-link expandohedra based on trivalent parents. The formulae are cast in terms of the numbers of links with C_2 site symmetry. A generic breathing expansion mode has been identified for all double-link expandohedra based on C_N-symmetric parent polyhedra and for all with non-zero numbers of links with C_2 site symmetry. The latter class includes double-link expandohedra based on trivalent platonic solids and crucially all those based on icosahedrally symmetric trivalent polyhedra with pentagonal and hexagonal faces only and with odd triangulation number. A potential expansion mechanism is thus identified for odd-T icosahedral viruses.

Numerical calculations on the structures defined by the first 15 triangulation numbers show the completeness of the generic symmetry treatment, from which it

can be deduced that the totally symmetric expansion mode is finite in all cases with odd $T \leq 31$, and non-existent in all cases with even $T \leq 36$. It is conjectured that these two results generalise to all T.

The research reported here was partially supported by the Royal Society through their European Exchange Programme. Partial support by OTKA Grant No. T031931 and FKFP Grant No. 0177/2001 is also gratefully acknowledged. SDG acknowledges the support of the Leverhulme Trust.

References

Atkins, P. W., Child, M. S. & Phillips, C. S. G. 1970 *Tables for Group Theory.* Oxford University Press.

Caspar, D. L. D. & Klug, A. 1962 Physical Principles in the Construction of Regular Viruses. *Cold Spring Harbor Symp. Quant. Biol.* **27**, 1–24.

Ceulemans, A. & Fowler, P. W. 1991 Extension of Euler's theorem to the symmetry properties of polyhedra. *Nature* **353**, 52–54.

Coxeter, H. S. M. 1972 Virus macromolecules and geodesic domes. In *A spectrum of mathematics* (ed. J.C. Butcher). Oxford University Press/Auckland University Press pp. 98–107.

Douglas, T. & Young, M. 1998 Host-guest encapsulation of materials by assembled virus protein cages. *Nature* **393**, 152–155.

Douglas, T. and Young, M., 1999. Virus particles as templates for materials synthesis. *Adv. Mater.* **11**, 679–681.

Fowler, P. W. & Steer, J. I. 1987 The leapfrog principle: A rule for electron counts of carbon clusters. *J. Chem. Soc. Chem. Comm.* **18**, 1403–1405.

Fowler, P. W. & Guest, S. D. 2000 A symmetry extension of Maxwell's rule for rigidity of frames. *Int. J. Solids Struct.* **37**, 1793–1804.

Fowler, P. W. & Guest, S. D. 2002 Symmetry Analysis of the double banana and related indeterminate structures. In *New Approaches to Structural Mechanics, Shells and Biological Structures* (ed. Drew H.R. & Pellegrino, S.). Kluwer Academic Publishers, pp. 91–100.

Fricks, C. E. & Hogle, J. M. 1990 Cell induced conformational changes in poliovirus: externalization of the amino terminus of VP1 is responsible for liposome binding. *J. Virol.* **64**, 1934–1945.

Goldberg M. 1937. A class of multi-symmetric polyhedra. *Tôhoku Math. J.* **43**, 104–108.

Guest, S. D. & Fowler, P. W. 2003 A symmetry-extended mobility rule. Submitted to *Mech. Mach. Theory.*

Hunt, K. H. 1978 *Kinematic Geometry of Mechanisms.* Oxford: Clarendon Press.

Kangwai, R. D. & Guest, S. D. 1999 Detection of finite mechanisms in symmetric structures. *Int. J. Solids Struct.* **36**, 5507–5527.

Kangwai, R. D. & Guest, S. D. 2000 Symmetry adapted equilibrium matrices. *Int. J. Solids Struct.* **37**, 1525–1548.

Kovács, F., Tarnai, T., Fowler, P. W. & Guest, S.D. 2003 A class of expandable polyhedral structures. Submitted to: *Int. J. Solids Struct.*

Manolopoulos, D. E. & Fowler, P.W., 1992. Molecular graphs, point groups and fullerenes. *J. Chem. Phys.* **96**, 7603–7614.

Pellegrino, S., 1993. Structural computations with the singular value decomposition of the equilibrium matrix. *Int. J. Solids Struct.* **30**, 3025–3035.

Pellegrino, S. & Guest, S. D. 2000 *Proc. IUTAM-IASS Symposium on Deployable Structures, Cambridge, UK, 60-9 September, 1998.* Kluwer Academic Publishers.

Rayment, I., Johnson J. E. & Rossman, M. G. 1979 Metal-free southern bean mosaic virus crystals. *J. Biol. Chem.* **254**, 5243–5245.

Robinson I. K. & Harrison S. C. 1982 Structure of the expanded state of tomato bushy stunt virus. *Nature* **297**, 563–568.

Sorger, P. K., Stockley, P. G. & Harrison, S. C. 1986 Structure and assembly of turnip crinkle virus II. Mechanism of reassembly in vitro. *J. Mol. Biol.* **191**, 693–658.

Speir, J. A., Munshi, S., Wang, G., Baker, T. S. & Johnson, J. E. 1995 Structures of the native and swollen forms of cowpea chlorotic mottle virus determined by X-ray crystallography and cryo-electron microscopy. *Structure* **3**, 63–78.